Electronic Supplementary Material (ESI) for Catalysis Science & Technology.
This journal is © The Royal Society of Chemistry 2014

Electronic Supplementary Information

for

A composite photocatalyst of an organic electron donor-acceptor dyad and a Pt catalyst supported on semiconductor nanosheets for efficient hydrogen evolution from oxalic acid

Yusuke Yamada, Akifumi Nomura, Hideyuki Tadokoro and Shunichi Fukuzumi*

Department of Material and Life Science, Graduate School of
Engineering, Osaka University, ALCA, Japan Science and Technology
Agency (JST), Suita, Osaka 565-0871, Japan

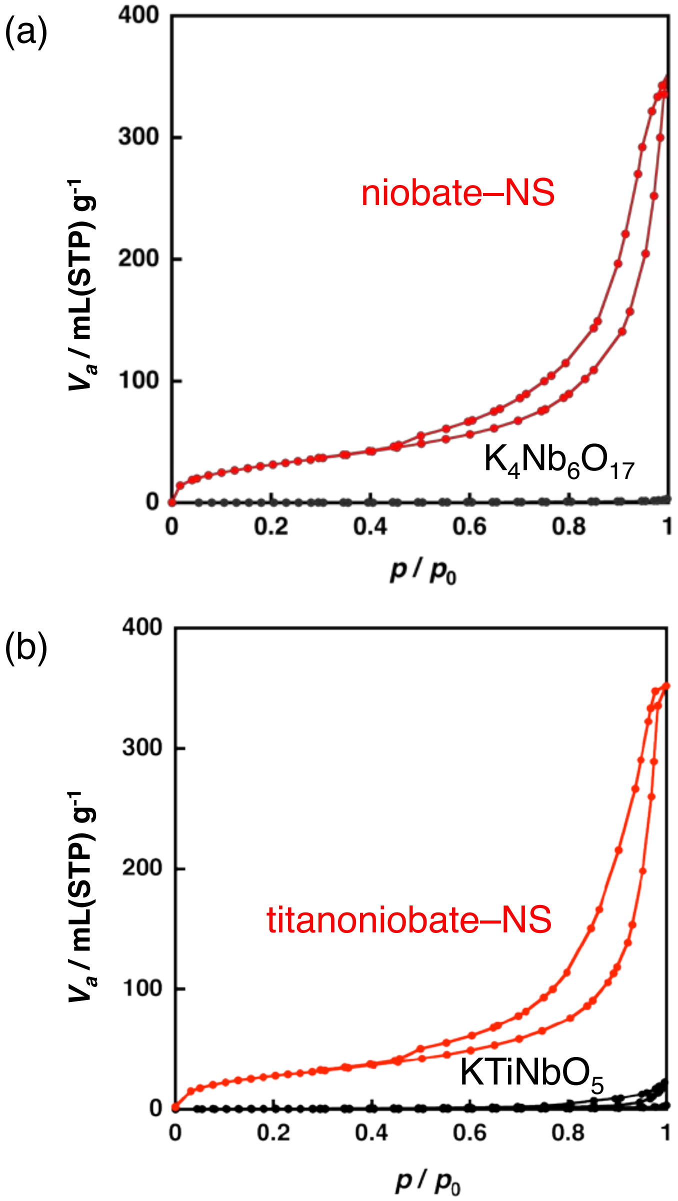

Fig. S1 Nitrogen adsorption-desorption isotherms of (a) $K_4Nb_6O_{17}$ and niobate-NS and (b) $KTiNbO_5$ and titanoniobate-NS at –196 °C.

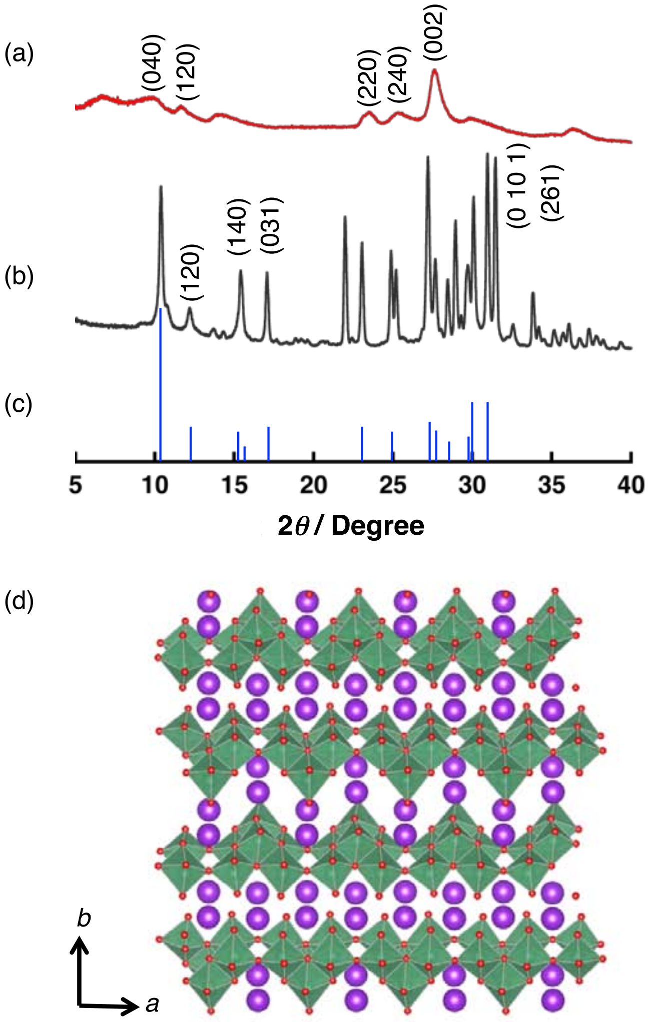

Fig. S2 Powder X-ray diffraction patterns of $K_4Nb_6O_{17}$ in the form of (a) nanoscroll and (b) layered oxide (as-prepared). (c) Peak positions and intensities indicated in literature.[S1] (d) Schematic drawings of crystal structure. NbO_6 units are indicated by green octahedra with red dots and K ions are indicated by purple circles.[S2]

(S1) A. D. Wadsley, *Acta Cryst.,* 1964, **17**, 623.
(S2) K. Momma and F. Izumi, *J. Appl. Crystallogr.,* 2011, **44**, 1272.

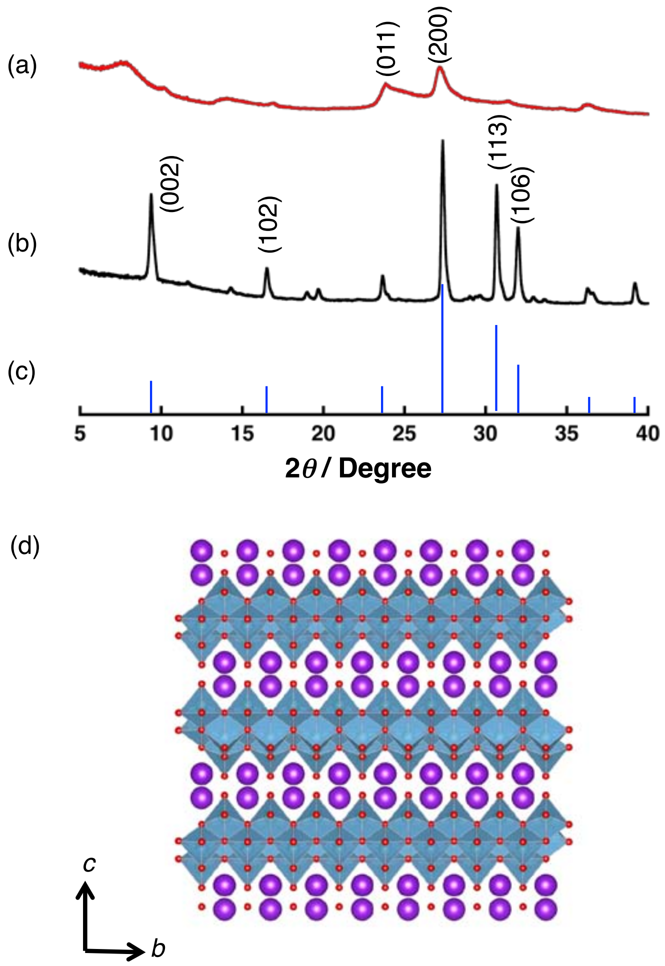

Fig. S3 Powder X-ray diffraction patterns of $KTiNbO_5$ in the form of (a) nanoscroll and (b) layered oxide (as-prepared). (c) Peak positions and intensities indicated in literature.[S3] (d) Schematic drawings of crystal structure. TiO_6 or NbO_6 units are indicated by blue octahedra with red dots and K ions are indicated by purple circles.[S2]

(S3) G. H. Du, Y. Yu, Q. Chen, R. H. Wang, W. Zhou and L. M. Peng, *Chem. Phys. Lett.,* 2003, **377**, 445.

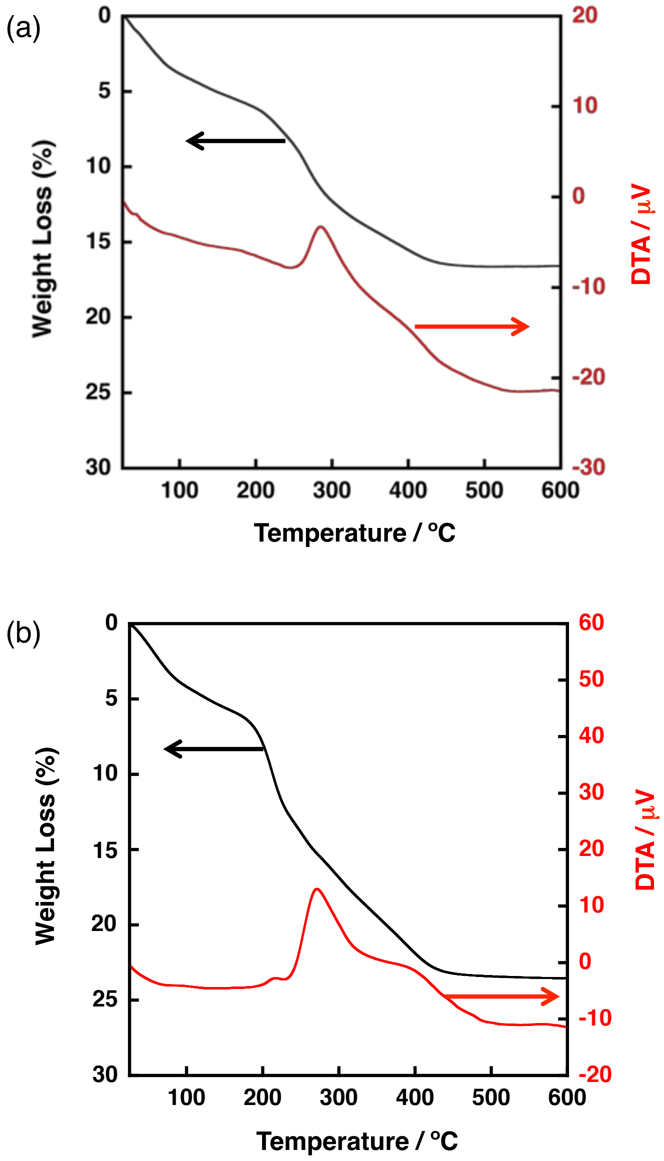

Fig. S4 TG/DTA curves of (a) niobate-NS and (b) titanoniobate-NS at temperature ranging from 20 °C to 600 °C.

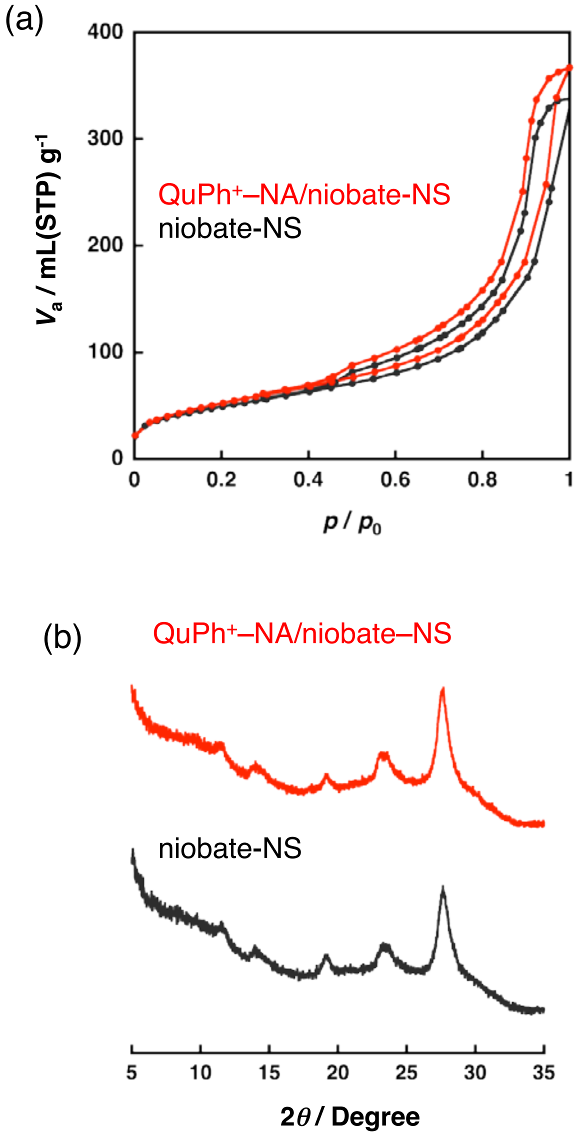

Fig. S5 (a) Nitrogen adsorption-desorption isotherms at -196 °C and (b) powder X-ray diffraction of QuPh$^+$–NA/niobate-NS (red) and niobate-NS (black).

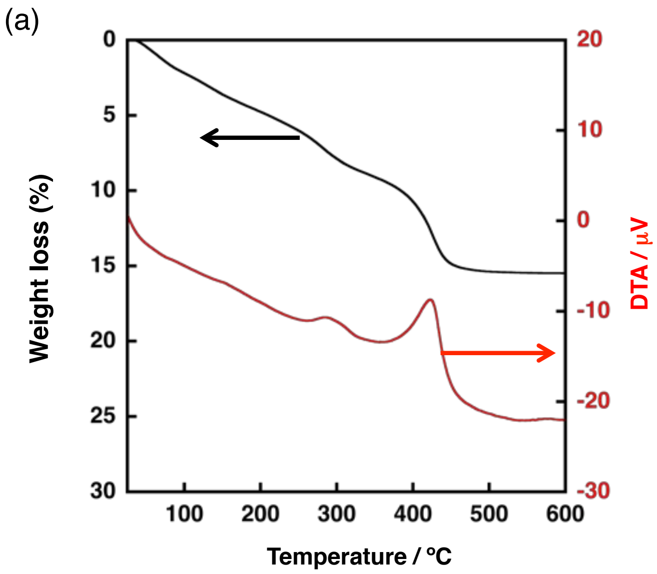

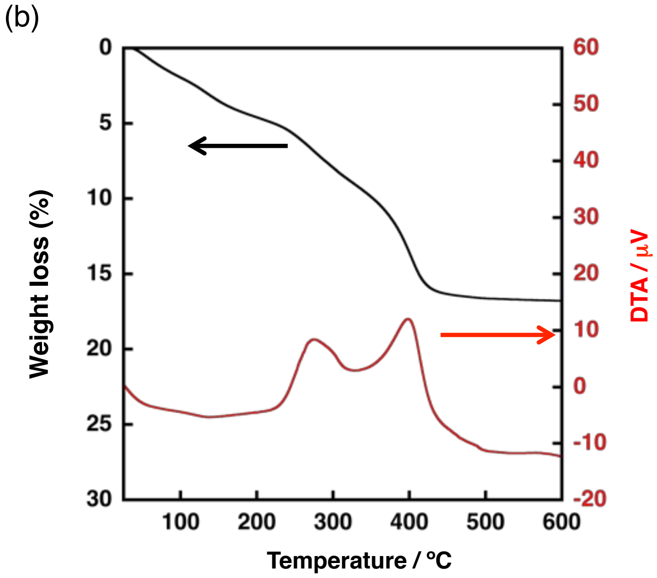

Fig. S6 TG/DTA curves of (a) QuPh$^+$–NA/niobate-NS and (b) QuPh$^+$–NA/titanoniobate-NS at temperature ranging from 20 °C to 600 °C.

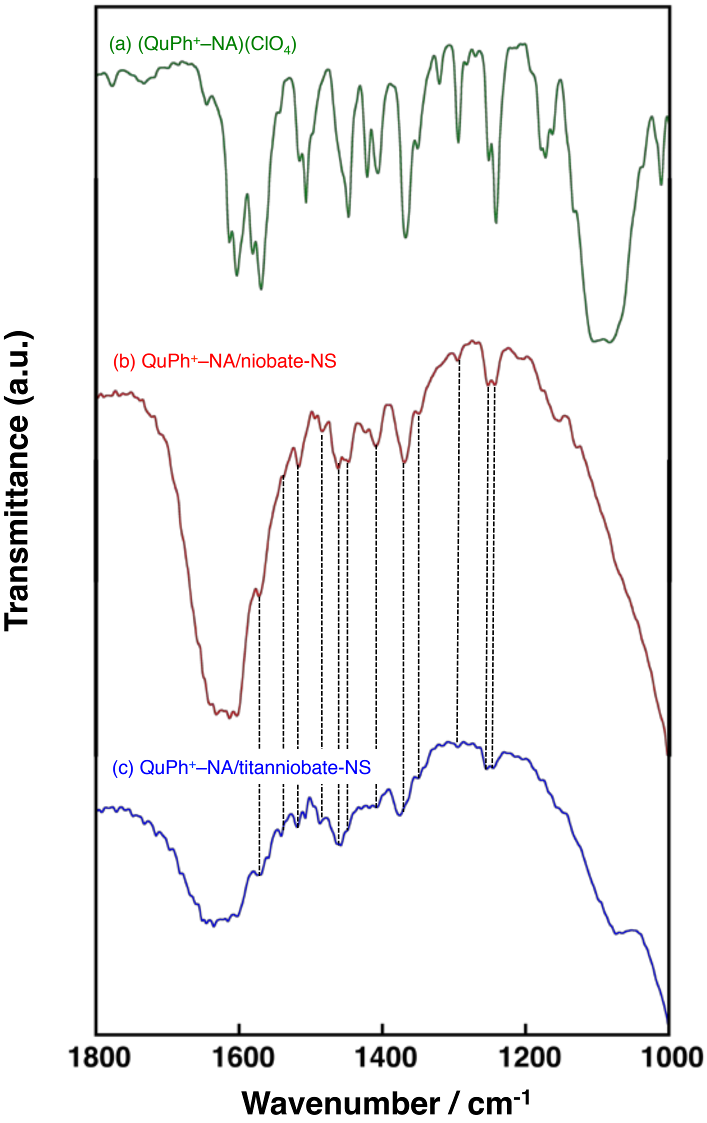

Fig. S7 IR absorption spectra of (a) (QuPh$^+$–NA)(ClO$_4$), (b) QuPh$^+$–NA/niobate-NS and (c) QuPh$^+$–NA/titanoniobate-NS. The samples were pelletized under pressurized conditions after mixing with KBr. The IR spectra were taken on a Jasco FT/IR-6200 spectrometer with the resolution of 4 cm^{-1}.

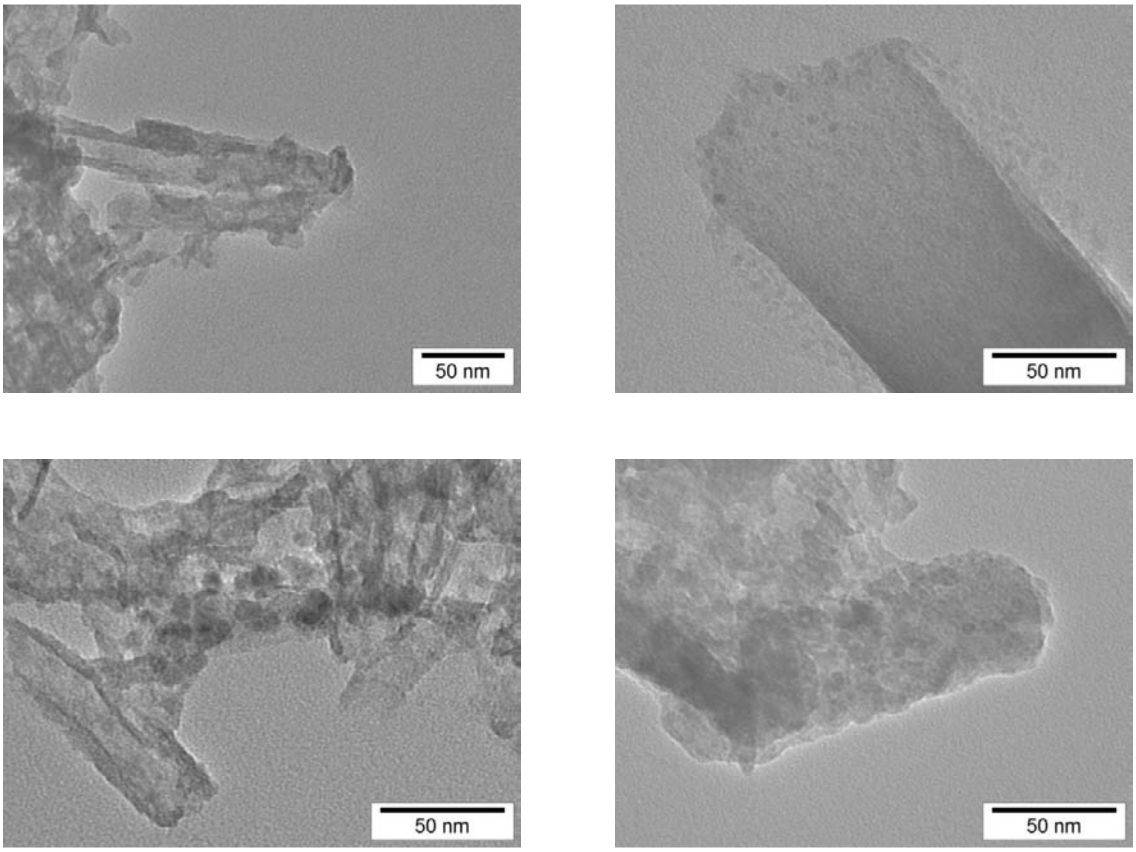

Fig. S8 TEM images of QuPh$^+$–NA/niobate-NS after the photoirradiation for 19 h in the presence of oxalic acid and $[Pt(NH_3)_4]^{2+}$.

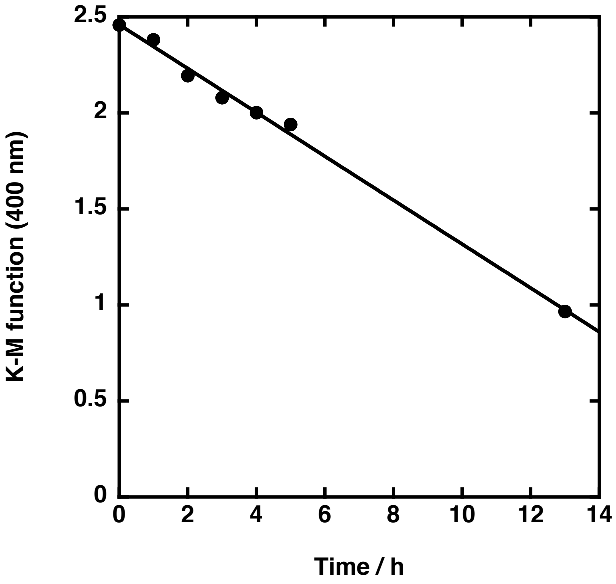

Fig. S9 Time course of absorbance of QuPh$^+$–NA/niobate-NS at 400 nm during the photocatalytic H_2 evolution.

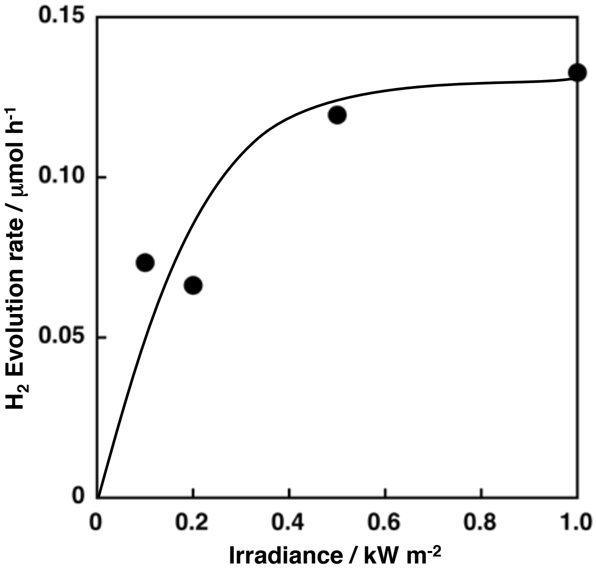

Fig. S10 H_2-evolution rates depending on the irradiance of a solar simulator (AM 1.5G). The photocatalytic H_2 evolution was performed by photoirradiation of an N_2-saturated aqueous suspension (2.mL) containing oxalic acid (50 mM), K_2PtCl_4 (10 µM) and QuPh$^+$–NA/niobate-NS (11.6 mg) using an HAL-320 solar simulator (Asahi spectra, AM 1.5G). The irradiance for each reaction was determined by a CS-20 irradiation meter (Asahi spectra).

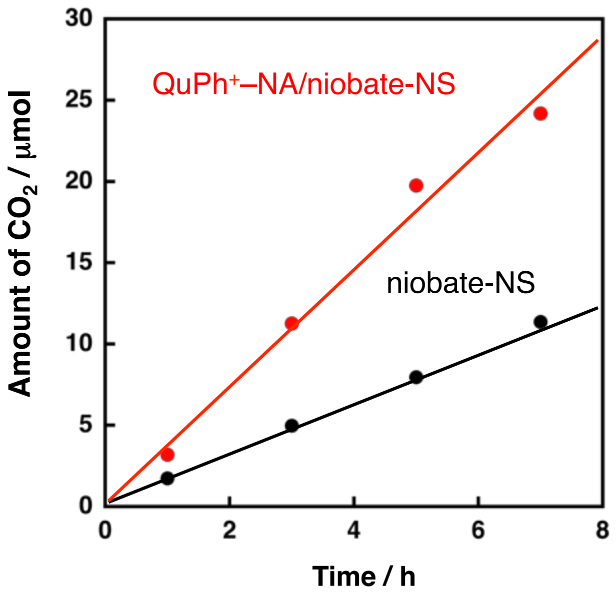

Figure S11 Time courses of CO_2 evolution by photoirradiation (λ > 340 nm) of an O_2-saturated aqueous suspension (2.0 mL, pH 1.4) containing oxalic acid (50 mM) and niobate-NS (11.6 mg, black) and $QuPh^+$–NA/niobate-NS (11.6 mg, red).